SAND2020-9108C

Lateral Inhibition and Winner-Take-All in Domain Wall Racetrack Arrays for Neuromorphic Computing

***Abstract*—Neuromorphic computing is a promising candidate for beyond-von Neumann computer architectures, featuring low power consumption and high parallelism. Lateral inhibition and winner-take-all (WTA) features play a crucial role in neuronal competition of the nervous system as well as neuromorphic hardwares. The domain wall - magnetic tunnel junction (DW-MTJ) neuron is an emerging spintronic artificial neuron device exhibiting intrinsic lateral inhibition. In this paper we show that lateral inhibition parameters effectively modulates the neuron firing statistics in a DW-MTJ neuron array, thus emulating *soft*-winner-take-all (WTA) and firing group selection.**

***Index Terms*—magnetism, spintronics, lateral inhibition, winner-take-all, domain wall racetrack, spin-transfer torque, neuromorphic computing**

I. Introduction

Inspired by the signal processing of the brain, neuromorphic computing exceeds classical von Neumann computers in terms of speed and power efficiency, particularly in data-intensive artificial intelligence applications [1] [2]. In the brain, neurons communicate through spikes and function as both the computational and data storage units; synapses store the weights of neuron connectivity and can be adjusted by learning. Numerous CMOS-based neuromorphic hardware have been proposed [3] [4] [5], but they lack the biological plausibility required to realize the full potential of neuromorphic circuits and networks [6].

Spintronic devices are known for their small footprints, high endurance, low power consumption and the highly tunable spin dynamics that are non-linear, stochastic and non-volatile, thus offering a new arena for neuromorphic device development [7]. Spintronic neuromorphic devices are closely modeled after their biological counterparts in both structure and functionality, leveraging non-volatility, non-linearity, stochasticity, and phenomena such as synchronization for efficient computing [8] [9] [10]. They have been shown to emulate the integrate-and-fire (IF) neurons [11], resonate-and-fire neurons [12] and memristive synapses [13].

However, unsupervised learning algorithms require additional functions such as winner-take-all (WTA) [14], and it is desirable that spintronic neurons and synapses incorporate such features. Here we present a simulation study of an important neuron functionality, *lateral inhibition*, in an array of domain wall-magnetic tunnel junction (DW-MTJ) neurons. While it has been proposed that an array of co-integrated DW-MTJ synapses and neurons can perform online learning by combining plastic synapse updates with the behavior of interacting neurons [15], and that this approach can achieve natural clustering or unsupervised learning on small tasks [16], these results assumed a coarse-grained model of lateral interaction. In this study, we expand our understanding of lateral inhibition, informing new directions for optimized nanofabricated domain wall-magnetic tunnel junction (DW-MTJ) coupled neural arrays. We will show that lateral inhibition strength and neuron arrangement can modulate neuron firing statistics of the array, which may be a useful property in implementing unsupervised learning algorithms.

II. Neuronal Winner-Take-All and Lateral Inhibition

In the nervous system, neuronal competition results in the selective firings of a subset of the neuron population. It has great importance in generating meaningful sensory information representations in response to external stimuli; otherwise, an explosive epileptic state will occur [17] [18]. Neuronal competition is regulated by a winner-take-all (WTA) process, in which one or more neurons win out by suppressing the activities of other competitors.

Competitive neural networks incorporate the WTA function to choose one or more neurons that are best matched with the input stimuli; the chosen winners then participate in synaptic weight adaptation (*i.e.* learning) [19]. Various mathematical models of WTA have been proposed. The traditional *hard*-WTA selects only one neuron as the winner. Two less extreme versions of WTA, namely the *k*-WTA and *soft*-WTA, have superior computational power [20]. *k*-WTA allows $k > 1$ neurons to be chosen as winners. It is closer to the biological realism than *hard*-WTA since it supports "distributed representation", in which sensory information is not localized to one neuron but is instead encoded in a group of neurons [17] [21]. Like *k*-WTA, *soft*-WTA produces multiple winners; in addition, their outputs are analog and proportional to the strengths of stimuli. *Soft*-WTA allows all competitors to be updated based on their performances, and was shown to achieve higher accuracy in classification task than *hard*-WTA [22]. In unsupervised learning, *soft*-WTA can also enable efficient Hebbian learning [19] and autonomous pattern recognition [23].

Lateral inhibition describes the the mutual inhibition of the neurons belonging to the same layer and is a biologically plausible WTA mechanism. In visual, auditory and somatosensory cortices, lateral inhibition enhances the contrast of neighboring

Sandia National Laboratories is a multimission laboratory managed and operated by National Technology & Engineering Solutions of Sandia, LLC, a wholly owned subsidiary of Honeywell International Inc., for the U.S. Department of Energy's National Nuclear Security Administration under contract DE-NA0003525.

cells in the receptive fields [24]. Lateral inhibition in WTA circuits can be implicitly modeled by choosing proper transistor connections and biasing, or, in a biologically realistic manner, be explicitly mediated by an inhibitory interneuron [25] [26]. The WTA-via-lateral inhibition feature has been realized in CMOS VLSI [27] [28] [29] as well as in hybrid CMOS-memristor crossbar array [30]. However, these implementations require peripheral circuitry, large numbers of transistors and recurrent connections between the neurons, resulting in substantial chip area and energy cost, especially for large-scale networks. We will show below that in the spintronic artificial neuron, magnetostatic interaction results in efficient intrinsic lateral inhibition.

III. DW-MTJ Integrate-and-Fire Neuron with Intrinsic Lateral Inhibition

The domain wall - magnetic tunnel junction (DW-MTJ) neuron is an artificial IF neuron based on the three-terminal MTJ logic device [31]. It consists of a magnetic racetrack for DW motion and a MTJ for spike signal readout (Fig. 1). DW position and velocity in the racetrack encode neuron activity and the MTJ position defines the neuron firing point. During the *integration* phase (Fig. 1(a)), the current-driven DW propagates towards the MTJ due to spin-transfer torque (STT) or spin-orbit torque (SOT); once the DW passes under the MTJ, its magnetoresistance (MR) is switched low and an output current spike can be read out, emulating the *firing* of the neuron (Fig. 1(b)). Therefore, the neuron with higher DW velocity fires first and is more active. The DW-MTJ neuron has high energy efficiency [11] [32], and simulation studies have also shown that neuron leaking [33] and lateral inhibition [34] [35] can also be implemented without extra energy cost.

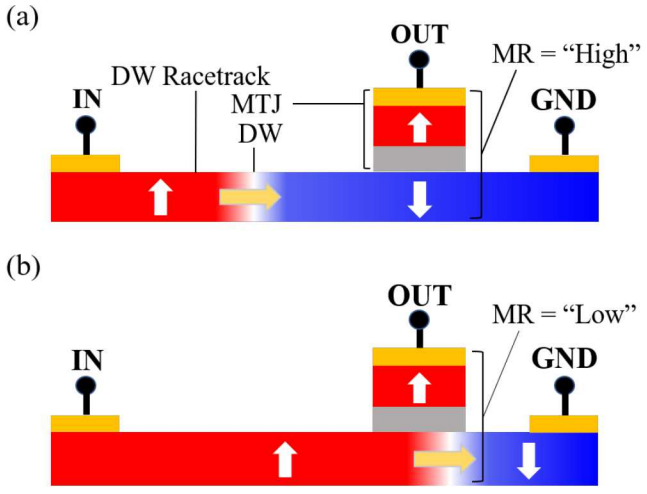

Fig. 1. Structure of the domain wall - magnetic tunnel junction (DW-MTJ) integrate-and-fire (IF) neuron. (a) integration: DW has not yet reached the firing point (MTJ) and the magnetoresistance (MR) state remains high. (b) fire: the DW is driven passed the firing point and the MR is switched low. A large output current ("spike") is generated.

Lateral inhibition of the DW-MTJ neuron is manifested in the enhanced DW velocity contrast: an active neuron delays or prevents the firing of its less active neighbor by further decreasing its DW velocity. According to the Landau-Lifshitz-Gilbert (LLG) equation and Walker's formulation of DW motion [36], DW velocity can be controlled by external magnetic field. The magnetostatic interaction between a pair of DW-MTJ neurons is shown in Fig. 2. Here, $\mathrm{DW_I}$ and $\mathrm{DW_N}$ propagate along $+x$ with DW velocities $v_{\mathrm{DWI}} < v_{\mathrm{DWN}}$. Neuron N exerts a stray field along $-z$ originating from its $+z$ domain on $\mathrm{DW_I}$; reciprocally, $\mathrm{DW_N}$ experiences a stray field along $+z$ originating from the $-z$ domain of Neuron I. It has been shown previously that the $-z$ stray field plays a central role in lateral inhibition, and by optimizing the stray field magnitude as well as the device geometrical and material parameters, an up to 90% reduction of $\mathrm{DW_I}$ velocity (i.e. 90% lateral inhibition) is achieved [35]. Since the DW-MTJ neuron is capable of performing lateral inhibition without electrical connections, the lateral inhibition implementation is energy efficient and scalable.

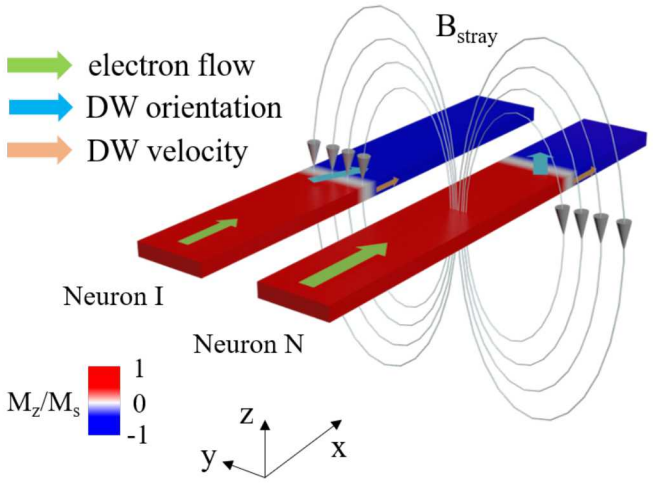

Fig. 2. Magnetostatic interaction and lateral inhibition of a pair of side-by-side DW-MTJ neurons (only DW racetracks are shown). Neuron N is more active and its stray field impedes the motion of $\mathrm{DW_I}$, resulting in lateral inhibition.

IV. Lateral Inhibition in DW-MTJ Neuron Arrays

Having established the basis of DW-MTJ neuron lateral inhibition, we now extend the discussion to the lateral inhibition of a DW-MTJ array. In a DW-MTJ array, a neuron experiences a complicated magnetic environment determined by input current configurations, and here we make the assumption that a neuron is only influenced by its two immediate neighbors. This assumption is justified by the rapid decrease of magnetic stray field at increased distances, as validated in [35]. Two types of neuron arrangements are considered: (a) the neurons are evenly arranged with nearest neighbor lateral distance s (Fig. 3(a)) and (b) the neurons are arranged with alternating lateral distances s_1 and s_2 ($s_1 < s_2$) (Fig. 3(b)). For arrangement (a), the two nearest neighbors contribute equally to the net stray field exerted on the center neuron. In this case, there is only

one inhibition condition (Case A): when both neighbors are more active than the center neuron. Only under such condition can it experience a field along $-z$; otherwise, the net stray field is either zero or along $+z$ because of the symmetry of the neighbor locations. Arrangement (b), on the other hand, allows for two inhibition conditions: Case B: the center neuron is less active than both neighbors, an equivalent of Case A; Case C: the center neuron is less active than its close neighbor N_1 but more active than its far neighbor N_2. As discussed in [35], inhibition strengths of Case B and C are generally different, and only one of them can be optimized by choosing s_1 and s_2.

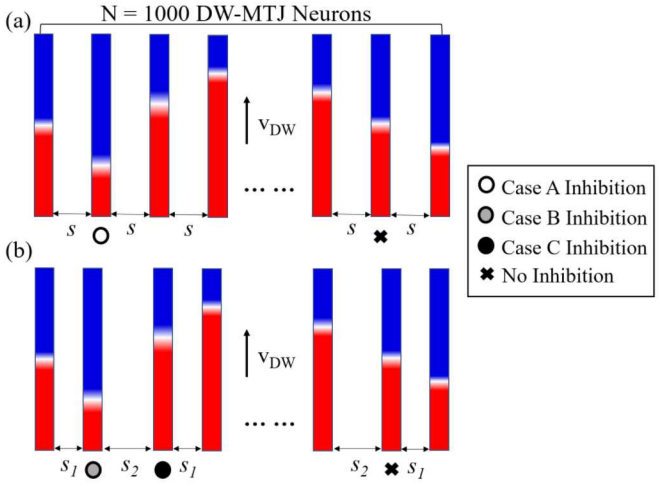

Fig. 3. DW-MTJ neuron arrangements in an array and lateral inhibition conditions. (a) Nearest neighbors are arranged with lateral distance s; (b) nearest neighbors are arranged with alternating lateral distances s_1 and s_2. Neurons with Case A, B, C inhibition and no inhibition are marked.

The DW-MTJ array investigated consists of $N = 1000$ neurons. We focus on the change of DW velocity distribution of the array due to lateral inhibition: $\{v_i\} \mapsto \{v_i'\}$, instead of the status of any specific neurons. A series of 1000 evenly distributed DW velocity values $\{v_i\}$ in the range $[v_{\min},\ v_{\max}] = [1,\ 3]$ (a.u. and proportional to input charge current densities) are randomly assigned to the neurons. For neuron arrangement (a), the inhibition strength of Case A is parameterized by the velocity reduction Δv_{A}; for neuron arrangement (b), inhibition strengths are parameterized by a pair $(\Delta v_{\mathrm{B}}, \Delta v_{\mathrm{C}})$ corresponding to Case B and C, respectively. $\{v_i'\}$ is calculated as follows:

$$\{v_i\} \mapsto \{v_i'\} : v_i' = \begin{cases} v_i - \Delta v_{\mathrm{A}}, & \text{for Case A inhibition} \\ v_i - \Delta v_{\mathrm{B}}, & \text{for Case B inhibition} \\ v_i - \Delta v_{\mathrm{C}}, & \text{for Case C inhibition} \\ v_i & \text{otherwise} \end{cases}$$

The calculated $\{v_i'\}$ are ranked in ascending order to yield the modified velocity distribution due to lateral inhibition. The values of Δv determine whether the inhibition causes the DW velocity signs to change:

$$\forall\, \Delta v \in \{\Delta v_{\mathrm{A}},\ \Delta v_{\mathrm{B}},\ \Delta v_{\mathrm{C}}\} < v_{\min},\ \textit{weak}\ \text{inhibition}$$
$$\exists\, \Delta v \in \{\Delta v_{\mathrm{A}},\ \Delta v_{\mathrm{B}},\ \Delta v_{\mathrm{C}}\} \geq v_{\min},\ \textit{strong}\ \text{inhibition}$$

We first study the *weak* inhibition. $\{v_i'\}$ are calculated with inhibition strengths Δv_A, Δv_B, Δv_C summarized in Table.1. Fig. 4(a) compares the $\{v_i'\}$ due to lateral inhibition for neuron arrangements (a) (solid lines) and (b) (dashed lines). For both types of arrangements, lowering of DW velocities from $\{v_i\}$ to $\{v_i'\}$ becomes more significant with larger inhibition strength. Notably, arrangement (a) results in non-linear $\{v_i'\}$: the low-velocity range shows the largest overall reduction, while the high-velocity range remains largely unchanged. This is due to the larger inhibition probability of the low-velocity (inactive) DWs, consistent with the inhibition mechanism described above. The non-linearity of the $\{v_i'\}$ increases with stronger inhibition. Arrangement (b), on the other hand, largely maintains the linearity of $\{v_i'\}$, since it improves the uniformity of inhibition probability across the whole DW velocity range as compared to arrangement (a). As visible, the weak inhibition does not strictly prohibit the firing of any members of the neuron array, but instead delays the firing of its inactive members.

TABLE I
INHIBITION STRENGTHS

Weak inhibition (Fig. 4(a))		
Arrangement (a)	Δv_A	$\{0.9, 0.7, 0.5, 0.3, 0.1\}$
Arrangement (b)	Δv_B	$\{0.9, 0.7, 0.5, 0.3, 0.1\}$
	Δv_C	$\{0.8, 0.6, 0.4, 0.2, 0\}$
Strong inhibition (Fig. 4(b))		
Arrangement (a)	Δv_A	$\{2.5, 2.2, 1.9, 1.6, 1.3, 1.0\}$
Arrangement (b)	Δv_B	$\{2.5, 2.2, 1.9, 1.6, 1.3, 1.0\}$
	Δv_C	$\{2.4, 2.1, 1.8, 1.5, 1.2, 0.9\}$

We next study the *strong* inhibition. We again calculate $\{v_i'\}$ with inhibition strengths summarized in Table. 1, with results plotted in Fig. 4(b). In this case, the distribution of $\{v_i'\}$ of both arrangements (a) and (b) are highly non-linear due to the large inhibition strength, and as in the *weak* inhibition case, arrangement (b) more effectively reduces the overall DW velocities than the arrangement (b). Negative v_i''s indicate that the corresponding members are prohibited from firing. We calculate the neuron firing proportion ($E\%$) of the array from the $\{v_i'\}$ of Fig. 4(b), shown in Fig. 4(c). The firing proportion $E\%$ is less than unity when $\Delta v_{\mathrm{A}}(\Delta v_{\mathrm{B}})$ is larger than $v_{\min}$ and monotonically decreases as inhibition strength becomes larger. The effect is more prominent for neuron arrangement (b), with $E\%$ as low as 53%.

Using a simple inhibition model with nearest neighbor coupling assumption, we are able to show the relation between neuron activity, firing statistics and lateral inhibition strengths. We can draw a direct comparison between *weak* inhibition and *soft*-WTA, and between *strong* inhibition and *k*-WTA. When inhibition is weak, all neurons in the array are allowed to

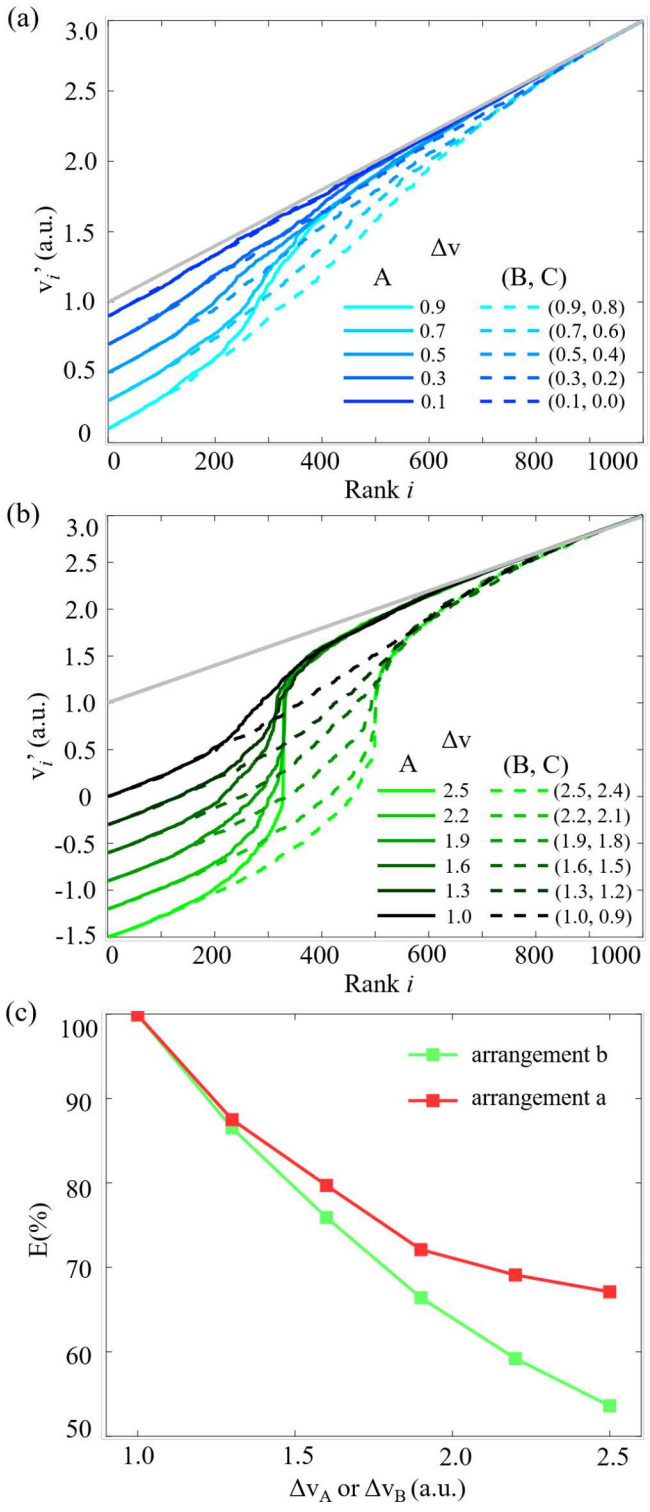

Fig. 4. DW velocity distribution change $\{v_i\} \mapsto \{v_i'\}$ due to lateral inhibition in an array of N = 1000 DW-MTJ neurons. (a) weak inhibition and (b) strong inhibition. Solid lines: arrangement (a); dashed lines: arrangement (b). $\{v_i\}$ are plotted in grey solid lines in both (a) and (b). (c) Neuron firing proportion $E\%$ versus inhibition strength, calculated from (b). Red: arrangement (a); green: arrangement (b). For the definitions of parameters Δv_A, Δv_B and Δv_C see text.

fire, but the DW velocity contrast in the array is enhanced by lateral inhibition. In this case, the activities or performances of the neurons can be inferred from their firing times. When inhibition is strong, besides delaying the firing of the inactive members of the array, it can forbid some of them from firing and thus control the neuron firing proportion of the array. It is also worth noting that the lateral inhibition of DW-MTJ neuron can be effectively tuned by field, current and device materials [35], which endows the neuron array with additional tunability that may be explored in future works.

V. Conclusions

We study the lateral inhibition and winner-take-all (WTA) characteristics of a DW-MTJ neuron array. Lateral inhibition of the DW-MTJ neuron arises from magnetostatic interaction, and modulates the WTA behaviors of the neuron array: a small inhibition strength lowers the overall DW velocities of the neuron members but does not prohibit their firing, mimicking the *soft*-WTA; a large inhibition strength reverses the motion of some DWs and strictly prohibits the corresponding neurons from firing, resulting in a firing proportion $E\%$ of down to 53% in our simulations, mimicking *k*-WTA. In addition, the WTA characteristics are also dependent on neuron arrangement: the non-evenly arranged neuron array yields a stronger overall inhibition than the evenly-arranged array. Our proposed lateral inhibition model provides a novel mechanism for implementing *soft*-WTA and group selection in spiking neural networks.

References

[1] P. A. Merolla, J. V. Arthur, R. Alvarez-Icaza, A. S. Cassidy, J. Sawada, F. Akopyan, B. L. Jackson, N. Imam, C. Guo, Y. Nakamura, and B. Brezzo, "A million spiking-neuron integrated circuit with a scalable communication network and interface," Science, vol. 345, pp. 668-673, 2014.

[2] P. Blouw, X. Choo, E. Hunsberger and C. Eliasmith, "Benchmarking keyword spotting efficiency on neuromorphic hardware," Neuro-inspired Computational Elements Workshop (NICE '19), 2019.

[3] G. Indiveri, E. Chicca and R. Douglas, "A VLSI array of low-power spiking neurons and bistable synapses with spike-timing dependent plasticity," IEEE Trans. Neural Netw., vol. 17, no. 1, pp. 211–221, 2006.

[4] J. S. Seo, B. Brezzo, Y. Liu, B. D. Parker, S. K. Esser, R. K. Montoye, B. Rajendran, J. A. Tierno, L. Chang, D. S. Modha and D. J. Friedman, "A 45nm CMOS neuromorphic chip with a scalable architecture for learning in networks of spiking neurons," 2011 IEEE Custom Integrated Circuits Conference (CICC) pp. 1-4, 2011.

[5] C. Frenkel, M. Lefebvre, J. D. Legat and D. Bol, "A 0.086-mm^2 12.7-pj/SOP 64k-synapse 256-neuron online-learning digital spiking neuromorphic processor in 28-nm CMOS," IEEE transactions on biomedical circuits and systems, vol. 13, no. 1, pp. 145-158, 2018

[6] C. S. Poon and K. Zhou, "Neuromorphic silicon neurons and large-scale neural networks: challenges and opportunities" Frontiers in neuroscience, vol. 5, pp. 108, 2011.

[7] J. Grollier, D. Querlioz and M. D. Stiles, "Spintronic nanodevices for bioinspired computing," Proceedings of the IEEE, vol. 104, no. 10, pp. 2024-2039, 2016.

[8] E. Kültürsay, M. Kandemir, A. Sivasubramaniam and O. Mutlu, "Evaluating STT-RAM as an energy-efficient main memory alternative," 2013 IEEE International Symposium on Performance Analysis of Systems and Software (ISPASS), pp. 256-267, 2013.

[9] A. F. Vincent, J. Larroque, N. Locatelli, N. B. Romdhane, O. Bichler, C. Gamrat, W. S. Zhao, J. O. Klein, S. Galdin-Retailleau and D. Querlioz, "Spin-transfer torque magnetic memory as a stochastic memristive synapse for neuromorphic systems," IEEE transactions on biomedical circuits and systems, vol. 9, no. 2, pp. 166-174, 2015.

[10] M. Romera et al., "Vowel recognition with four coupled spin-torque nano-oscillators," Nature, vol. 563, no. 7730, pp. 230-234, 2018.
[11] M. Sharad, C. Augustine, G. Panagopoulos and K. Roy, "Spin-based neuron model with domain-wall magnets as synapse," IEEE Trans. Nanotechnol., vol. 11, no. 4, pp. 843–853, Jul. 2012.
[12] M. A. Azam, D. Bhattacharya, D. Querlioz and J. Atulasimha, "Resonate and fire neuron with fixed magnetic skyrmions," Journal of Applied Physics, vol. 124, no. 15, p. 152122, 2018.
[13] S. Lequeux, J. Sampaio, V. Cros, K. Yakushiji, A. Fukushima, R. Matsumoto, H. Kubota, S. Yuasa and J. Grollier, "A magnetic synapse: multilevel spin-torque memristor with perpendicular anisotropy," Scientific reports, vol. 6, no. 1, pp. 1-7, 2016.
[14] B. M. Wilamowski, "Neural network architectures and learning," IEEE International Conference on Industrial Technology, vol. 1, pp. TU1-T12, 2003.
[15] C. H. Bennett, N. Hassan, X. Hu, J. A. C. Incorvia, J. S. Friedman and M. J. Marinella, "Semi-supervised learning and inference in domain-wall magnetic tunnel junction (DW-MTJ) neural networks," Spintronics XII, vol. 11090, p. 110903I, International Society for Optics and Photonics, 2019.
[16] A. Velasquez, C. H. Bennett, N. Hassan, W. H. Brigner, O. G. Akinola, J. A. C. Incorvia, M. J. Marinella and J. S. Friedman, "Unsupervised competitive hardware learning rule for spintronic clustering architecture," arXiv preprint, arXiv:2003.11120, 2020.
[17] R. C. O'Reilly, "Six principles for biologically based computational models of cortical cognition," Trends in cognitive sciences, vol. 2, no. 11, pp. 455-462, 1998.
[18] Y. Chen, "Mechanisms of winner-take-all and group selection in neuronal spiking networks," Frontiers in computational neuroscience, vol. 11, p. 20, 2017.
[19] A. Gupta and L. N. Long, "Hebbian learning with winner take all for spiking neural networks," 2009 International Joint Conference on Neural Networks, pp. 1054-1060, 2009.
[20] W. Maass, "On the computational power of winner-take-all," Neural computation vol. 12, pp. 2519-2535, 2000.
[21] T. Fukai and S. Tanaka, "A simple neural network exhibiting selective activation of neuronal ensembles: from winner-take-all to winners-share-all," Neural computation, vol. 9, no. 1, pp. 77-97, 1997.
[22] S. J. Nowlan, "Maximum likelihood competitive learning," Advances in neural information processing systems, pp. 574-582, 1990
[23] R. Kreiser, T. Moraitis, Y. Sandamirskaya and G. Indiveri, "On-chip unsupervised learning in winner-take-all networks of spiking neurons," 2017 IEEE Biomedical Circuits and Systems Conference (BioCAS), Turin, pp. 1-4, 2017.
[24] B. J. Baars and N. M. Gage, Cognition, Brain, and Consciousness. Cambridge: Academic Press, 2010.
[25] H. Mostafa, L. K. Muller and G. Indiveri, "Rhythmic inhibition allows neural networks to search for maximally consistent states," Neural computation, vol. 27, pp. 2510-2547, 2015.
[26] R. Coultrip, R. Granger and G. Lynch, "A cortical model of winner-take-all competition via lateral inhibition," Neural Networks vol. 5, pp. 47-54, 1992.
[27] M. Oster, Y. Wang, R. Douglas and S. C. Liu, "Quantification of a spike-based winner-take-all VLSI network," IEEE Transactions on Circuits and Systems I: Regular Papers, vol. 55, no. 10, pp. 3160-3169, 2008.
[28] J. Lazzaro, S. Ryckebusch, M. A. Mahowald and C. A. Mead, "Winner-take-all networks of O(N) complexity," Advances in neural information processing systems, pp. 703-711, 1989.
[29] J. Choi and B. J. Sheu, "A high-precision VLSI winner-take-all circuit for self-organizing neural networks," IEEE J. Solid-State Circuits, vol. 28, pp. 576-584, 1993.
[30] I. E. Ebong and P. Mazumder, "CMOS and memristor-based neural network design for position detection," Proceedings of the IEEE, vol. 100, pp. 2050-2060, 2011.
[31] J. A. Currivan-Incorvia, S. Siddiqui, S. Dutta, E. R. Evarts, J. Zhang, D. Bono, C. A. Ross and M. A. Baldo, "Logic circuit prototypes for three-terminal magnetic tunnel junctions with mobile domain walls," Nat. Commun., vol. 7, pp. 10275, 2016.
[32] A. Sengupta, Y. Shim and K. Roy, "Proposal for an all-spin artificial neural network: Emulating neural and synaptic functionalities through domain wall motion in ferromagnets," IEEE Trans. Biomed. Circuits Syst., vol. 10, pp. 1152-1160, 2016.
[33] W. H. Brigner, X. Hu, N. Hassan, C. H. Bennett, J. A. C. Incorvia, F. Garcia-Sanchez and J. S. Friedman, "Graded-anisotropy-induced magnetic domain wall drift for an artificial spintronic leaky integrate-and-fire neuron," IEEE J. Explor. Solid-State Computat., vol. 5, pp. 19-24, 2019.
[34] N. Hassan, X. Hu, L. Jiang-Wei, W. H. Brigner, O. G. Akinola, F. Garcia-Sanchez, M. Pasquale, C. H. Bennett, J. A. C. Incorvia and J. S. Friedman, "Magnetic domain wall neuron with lateral inhibition," Journal of Applied Physics, vol. 124, pp. 152127, 2018.
[35] C. Cui, O. G. Akinola, N. Hassan, C. H. Bennett, M. J. Marinella, J. S. Friedman, and J. A. C. Incorvia, "Maximized lateral inhibition in paired magnetic domain wall racetracks for neuromorphic computing," Nanotechnology, vol. 31, pp. 294001, 2020.
[36] N. L. Schryer and L. R. Walker, "The motion of 180° domain walls in uniform DC magnetic fields," J. Appl. Phys., vol. 45, pp. 5406-5421, 1974.